A bns347

(AGCTGCCGTTGGGCTTCAG>GAAACCACTC)
K1042R; L1043N; P1044_G1046del; F1047H; R1048S

Variant	PROVEAN Score	Prediction (Cutoff= -2.5)
K1042R	-1.437	Neutral
L1043N	-5.653	Deleterious
P1044_G1046del	-17.370	Deleterious
F1047H	-0.475	Neutral
R1048S	-5.008	Deleterious

B DNA sequence

```
WT      GAGGAACGCCGTACTGCGGGATGACCTGCGCTGAACTCTATGAGAAGCTGCCGTTGGGCT 60
        ||||||||||||||||||||||||||||||||||||||||||||||||||||| |    ||  | |
bns347  GAGGAACGCCGTACTGCGGGATGACCTGCGCTGAACTCTATGAGA-GAAACCACTCG--- 56

WT      TCAGGCTGGAGAAACCACTGAACT                                      84
            ||||||||||||||||||||
bns347  -----CTGGAGAAACCACTGAACT                                      75
```

C Protein sequence

```
WT      NVLVGENFVAKIADFGLSRGQEVYVKKTMGRLPVRWMAIESLNYSVYTTNSDVWSYGVLL 1019
bns347  NVLVGENFVAKIADFGLSRGQEVYVKKTMGRLPVRWMAIESLNYSVYTTNSDVWSYGVLL 1019
        ************************************************************

WT      WEVVSLGGTPYCGMTCAELYEKLPLGFRLEKPLNCDDEVYELMQQCWREKPFERPSFSQI 1079
bns347  WEVVSLGGTPYCGMTCAELYERN---HSLEKPLNCDDEVYELMQQCWREKPFERPSFSQI 1076
        **********************:    .  ********************************

WT      LLSLGRMLEERKTYVNTTLYEKFTYAGIDCSAEEAG                          1115
bns347  LLSLGRMLEERKTYVNTTLYEKFTYAGIDCSAEEAG                          1112
        ************************************
```

Figure S1. *tek*^{bns347} in-frame deletion is predicted to severely impair Tek function.

(A) The *tek*^{bns347} allele contains a 19 bp deletion (AGCTGCCGTTGGGCTTCAG) and a 10 bp insertion (GAAACCACTC) in exon 21, resulting in K1042R, L1043N, P1044_G1046 deletion, F1047H and R1048S in the TK domain; PROVEAN analysis indicates that this lesion is overall deleterious. (B) *tek*^{bns347} in-frame deletion as revealed by Sanger sequencing (partial sequence of exon 21 shown). (C) Amino acid sequence alignment of WT and Tek^{bns347} proteins.

A

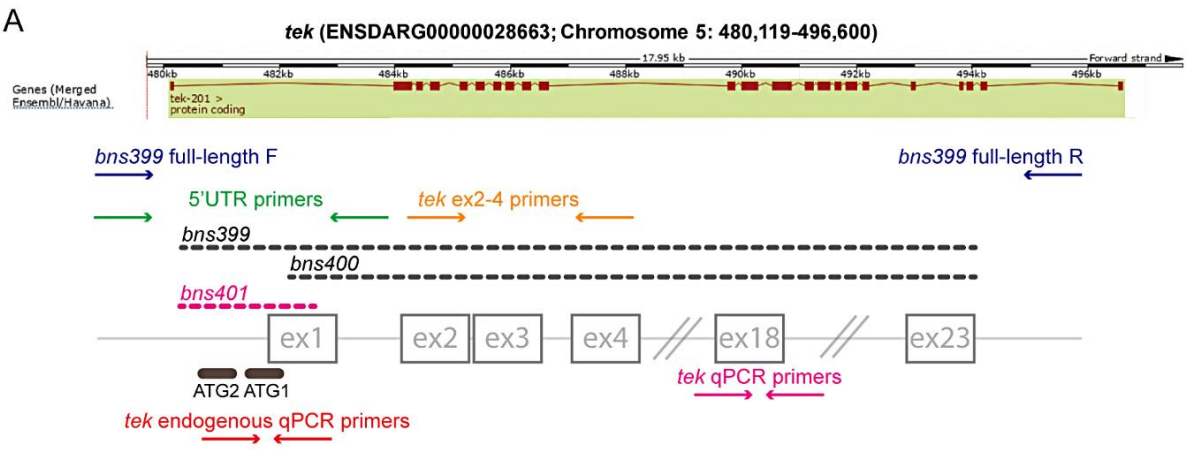

B

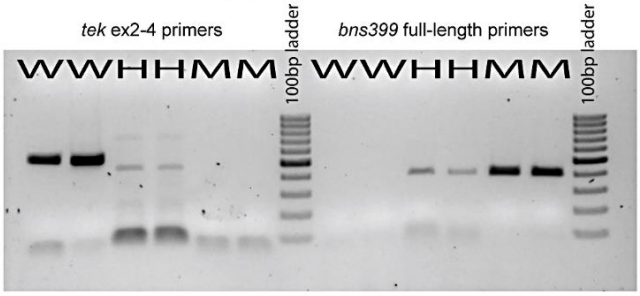

C

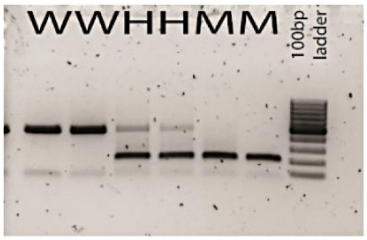

D

```
WT      CCCTGCAGGCTGGGTTACAGGAGGTCG  ...  GAGGAGGCCGGCTGATGCGCTGCCGCAAT
bns399  CCCTGCAGGCTGGGT------------          ------------GATGCGCTGCCGCAAT
        ***************  <-- 16733 bp deletion -->  ****************
```

E

```
WT      CCTGCAGGCTGGGTTACAGGAGGTCG  ...  CTGCTCTGCTGCTGCTCGGCTGCTGGA
bns401  CCTGCAGGCTGGGT------------          ------------TGCTCGGCTGCTGGA
        ***************  <-- 261 bp deletion -->  ***************
```

F bns401

Variant	PROVEAN Score	Prediction (Cutoff= -2.5)
M1_W16del	-2.067	Neutral

G Protein sequence

```
WT      MCLLDSCTALLLLGCWMSGSAVRISDVTLVNPDPVVSPLTAPSLLCVSSDWSSGGSVLAL   60
bns401  ----------------MSGSAVRISDVTLVNPDPVVSPLTAPSLLCVSSDWSSGGSVLAL   44
                        ************************************************

WT      GQEFPRPQGSVLALGQEFPHTEPRPHPAAATVTWSSRSHAFGAFYCQIRNSTGRKIYTYK   120
bns401  GQEFPRPQGSVLALGQEFPHTEPRPHPAAATVTWSSRSHAFGAFYCQIRNSTGRKIYTYK   104
        ************************************************************
```

Figure S2. Genotyping the *tek*^{bns399} RNA-less allele and the *tek*^{bns401} 5'UTR deletion allele, and location of relevant primers.

(A) *tek* locus based on Ensembl annotation and schematic positioning of the genotyping and RT-PCR primers (arrows), the MOs (bold solid lines), and the deletions (dashed lines). (B) Genotyping the *tek*^{bns399} RNA-less allele with different PCR primer sets to identify WT and mutant bands. (C) Genotyping the *tek*^{bns401} 5'UTR deletion allele by PCR. (D) Deletion in the *tek*^{bns399} RNA-less allele as revealed by Sanger sequencing. (E) Deletion in the *tek*^{bns401} allele as revealed by Sanger sequencing. (F) The *tek*^{bns401} allele contains a 261 bp deletion, resulting in M1_W16 deletion; PROVEAN analysis indicates that this lesion is overall neutral. (G) Amino acid sequence alignment of WT and Tek^{bns401} proteins.

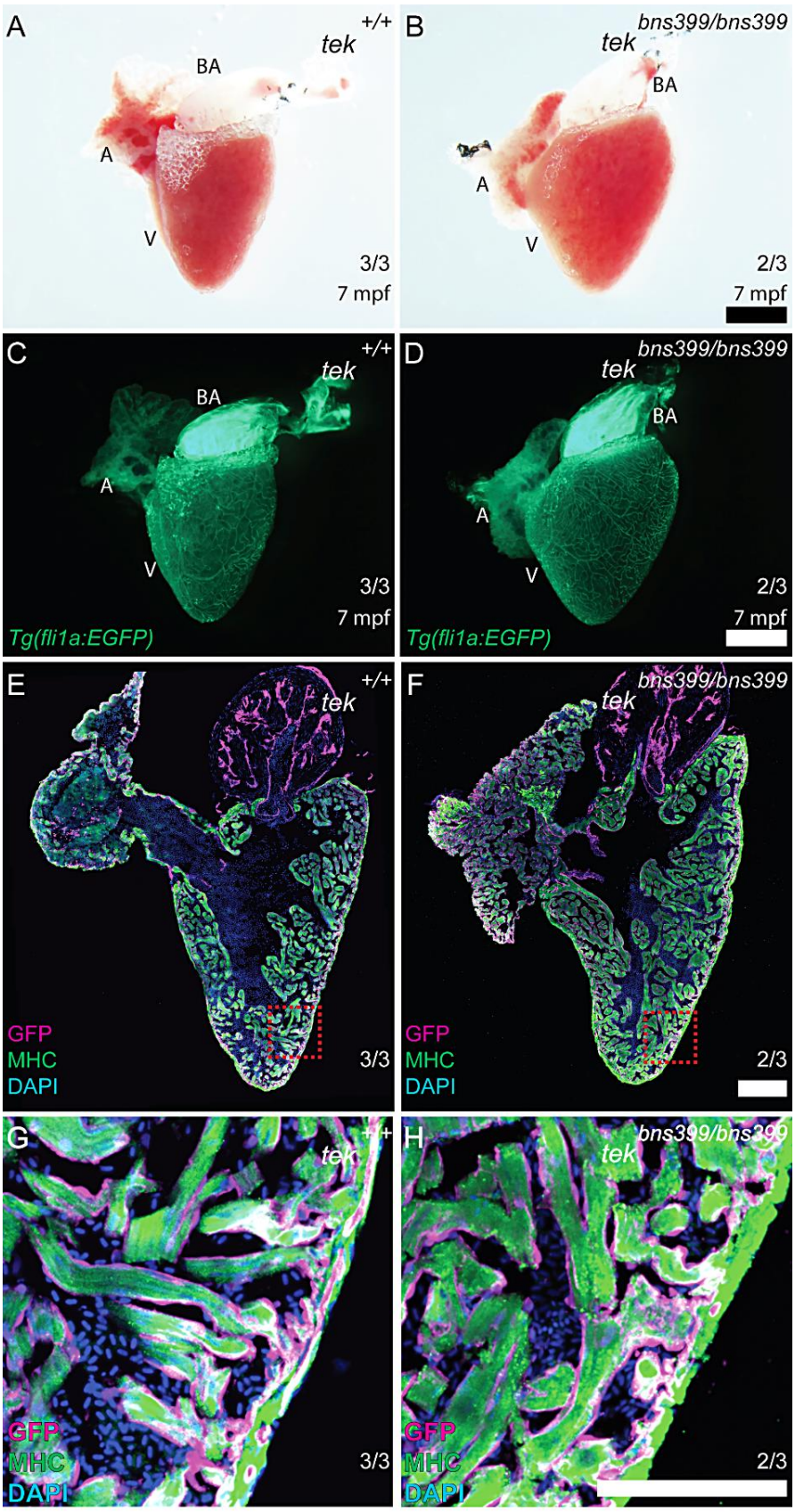

Figure S3. No obvious phenotypes in adult hearts of *tek*^{bns399} RNA-less mutants.

(A, B) Brightfield images of dissected hearts from 7 mpf +/+ siblings (A) and *tek*$^{bns399/bns399}$ animals (B). (C, D) Fluorescent images of coronary vessels in dissected hearts from 7 mpf *Tg(fli1a:EGFP)* +/+ siblings (C) and *tek*$^{bns399/bns399}$ animals (D). Scale bars: 500 μm. (E-H) Sections of dissected hearts from 7 mpf +/+ siblings (E, G) and *tek*$^{bns399/bns399}$ animals (F, H). Endothelial cells immunostained with anti-GFP (magenta), cardiomyocytes with anti-MHC antibody (green), and nuclei counterstained with DAPI (blue). (G, H) Magnified figures of red-boxed areas in panels E and F, respectively. Scale bars: 200 μm.

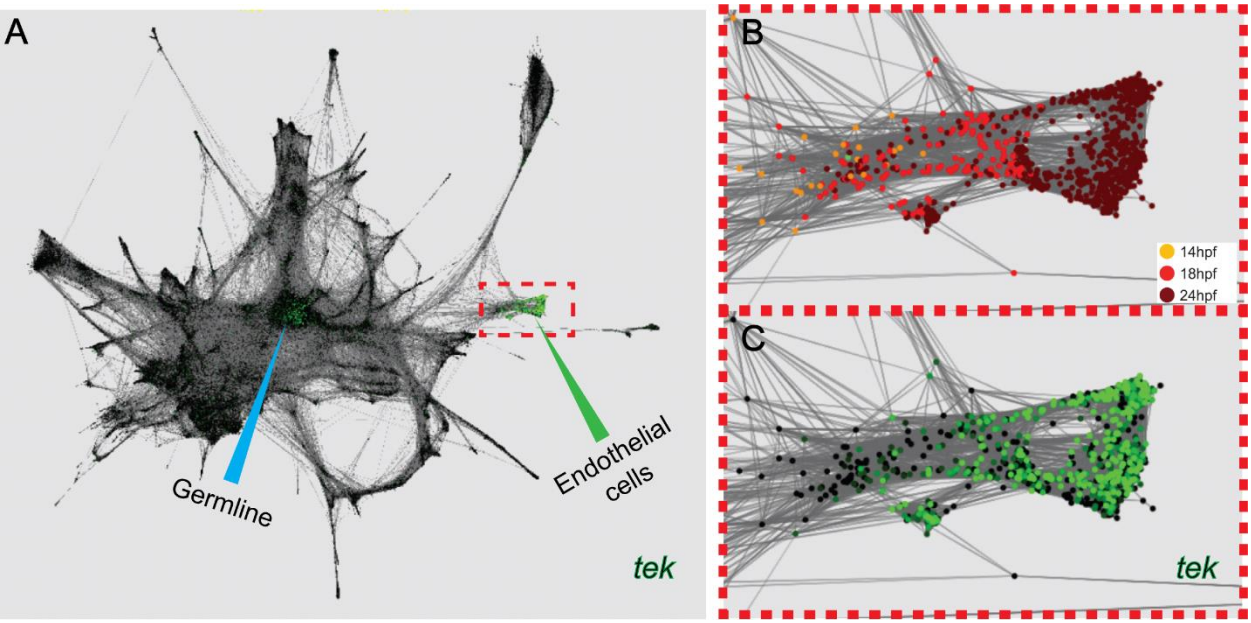

Figure S4. Embryonic expression of *tek* is highly enriched in endothelial cells.

(A) Overview of zebrafish *tek* expression in the single cell RNA-Seq dataset from the Klein lab (https://kleintools.hms.harvard.edu/paper_websites/wagner_zebrafish_timecourse2018/mainpage.html). *tek* positive cells are highlighted in green. (B) Magnified figure of the red boxed endothelial cell group from panel A, showing an overview of the zebrafish single cell RNA-Seq data at different time points. (C) *tek* expression is endothelial cell enriched.

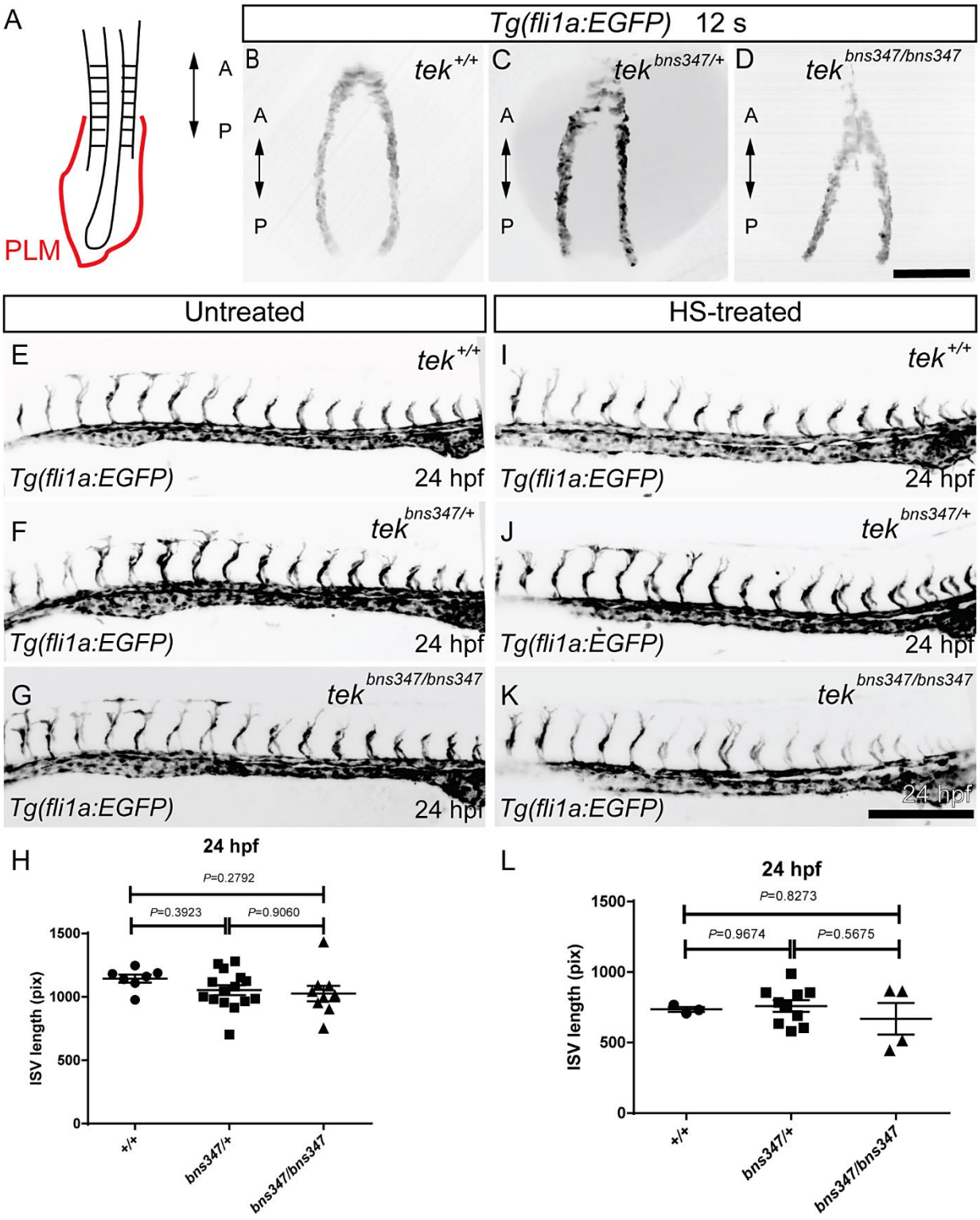

Figure S5. No obvious phenotypes in *tek*^{bns347} in-frame deletion mutants at early or late stages.

(A) Schematic representation of the posterior lateral plate mesoderm (PLM). (B-D) Dorsal views of the PLM in *tek*$^{bns347/+}$ incrossed embryos at the 12 somite-stage. (E-G) Lateral views of trunk vessels in 24 hpf *tek*$^{bns347/+}$ incrossed embryos. (H) Total length of 14 ISVs above the yolk extension in 24 hpf *tek*$^{bns347/+}$ incrossed embryos. (I-K) Lateral views of trunk vessels in 24 hpf *tek*$^{bns347/+}$ incrossed embryos heat-shocked (HS) at 10 and 22 hpf for 1 hour. (L) Total length of 14 ISVs above the yolk extension in 24 hpf *tek*$^{bns347/+}$ incrossed embryos heat-shocked at 10 and 22 hpf for 1 hour. In panels H and L, error bars represent means ± SD (by one-way analysis of variance (ANOVA) followed by Tukey's HSD test). Scale bars: 200 μm.

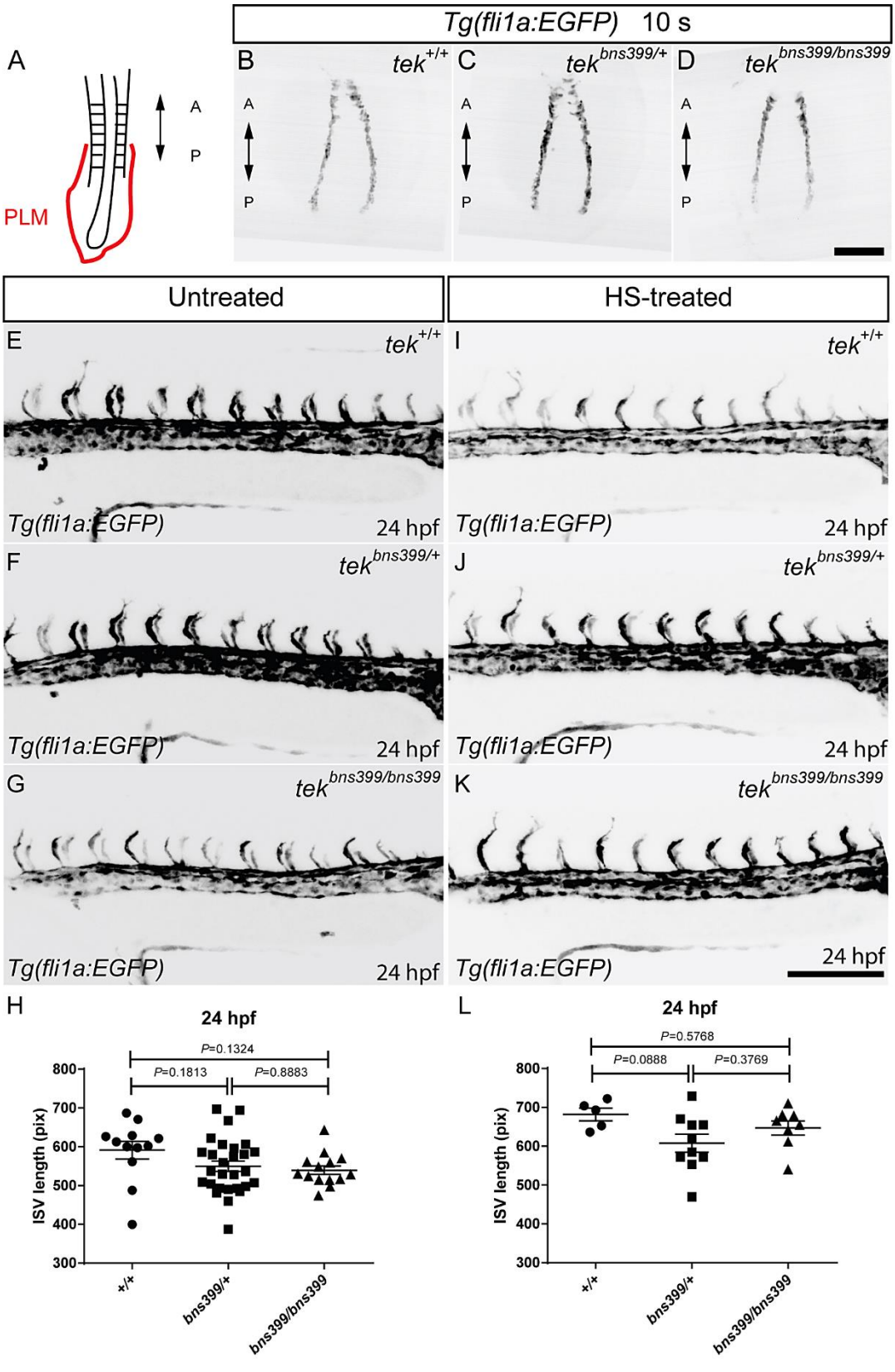

Figure S6. No obvious phenotypes in *tek*^{bns399} RNA-less mutants at early or late stages.

(A) Schematic representation of the posterior lateral plate mesoderm (PLM). (B-D) Dorsal views of the PLM in *tek*$^{bns399/+}$ incrossed embryos at the 10 somite-stage. (E-G) Lateral views of trunk vessels in 24 hpf *tek*$^{bns399/+}$ incrossed embryos. (H) Total length of 10 ISVs above the yolk extension in 24 hpf *tek*$^{bns399/+}$ incrossed embryos. (I-K) Lateral views of trunk vessels in 24 hpf *tek*$^{bns399/+}$ incrossed embryos heat-shocked (HS) at 10 and 22 hpf for 1 hour. (L) Total length of 10 ISVs above the yolk extension in 24 hpf *tek*$^{bns399/+}$ incrossed embryos heat-shocked at 10 and 22 hpf for 1 hour. In panels H and L, error bars represent means ± SD (by one-way analysis of variance (ANOVA) followed by Tukey's HSD test). Scale bars: 200 μm.

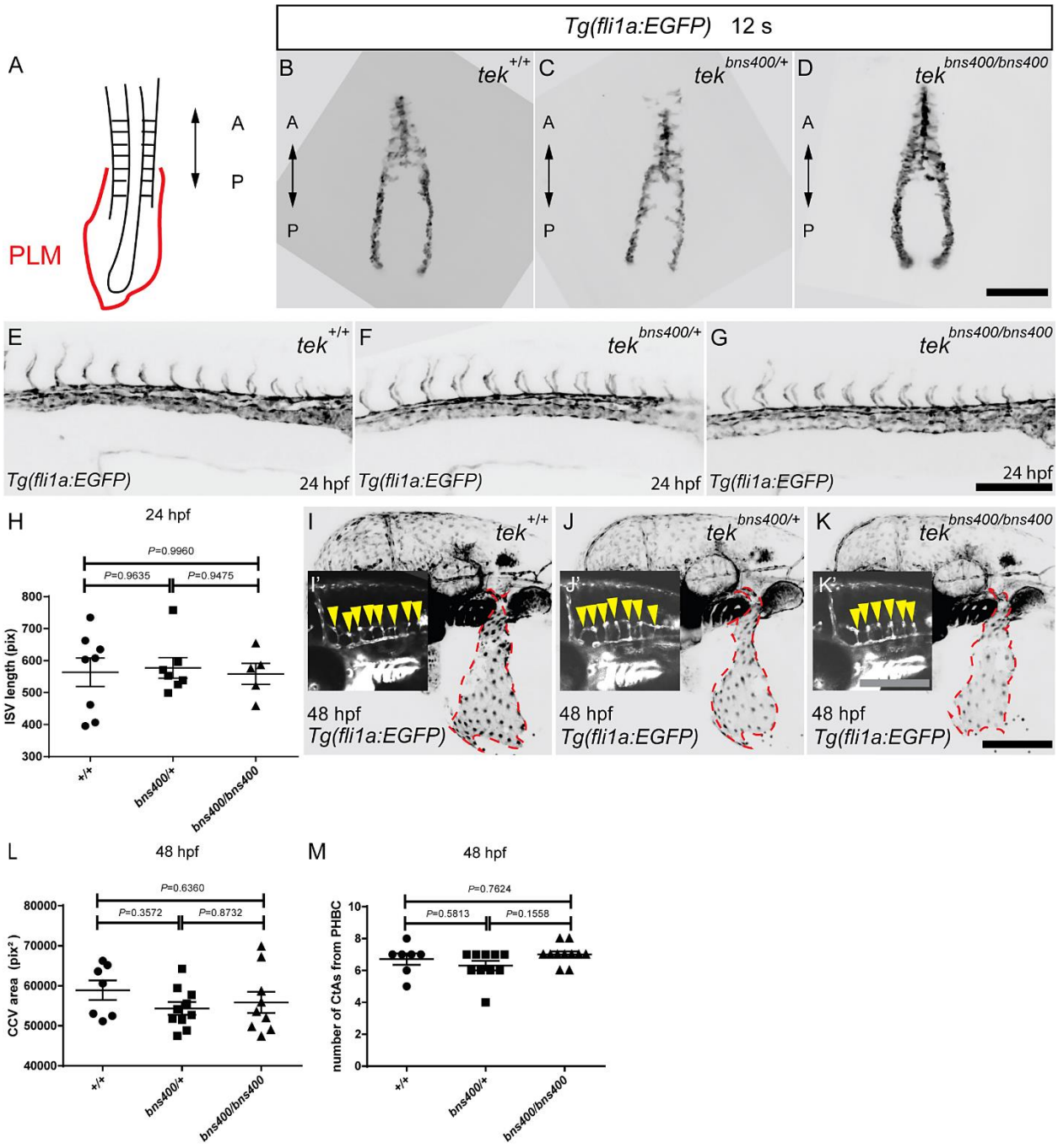

Figure S7. No obvious phenotypes in *tek*^{bns400} RNA-less mutants at early or late stages.

(A) Schematic representation of the posterior lateral plate mesoderm (PLM). (B-D) Dorsal views of the PLM in *tek*$^{bns400/+}$ incrossed embryos at the 12 somite-stage. (E-G) Lateral views of trunk vessels in 24 hpf *tek*$^{bns400/+}$ incrossed embryos. (H) Total length of 10 ISVs above the yolk extension in 24 hpf *tek*$^{bns400/+}$ incrossed embryos. (I-K) Lateral views of the head vasculature in 48 hpf *tek*$^{bns400/+}$ incrossed embryos. Red dashed lines outline the CCV. (I'-K') Lateral views of the head vessels in 48 hpf *tek*$^{bns400/+}$ incrossed embryos. Yellow arrowheads point to CtAs. (L) CCV area in 48 hpf *tek*$^{bns400/+}$ incrossed embryos. (M) CtA numbers in *tek*$^{bns400/+}$ incrossed embryos at 48 hpf. CtA: Central Artery; CCV: Common Cardinal Vein. In panels H, L and M, error bars represent means ± SD (by one-way analysis of variance (ANOVA) followed by Tukey's HSD test). Scale bars: 200 μm.

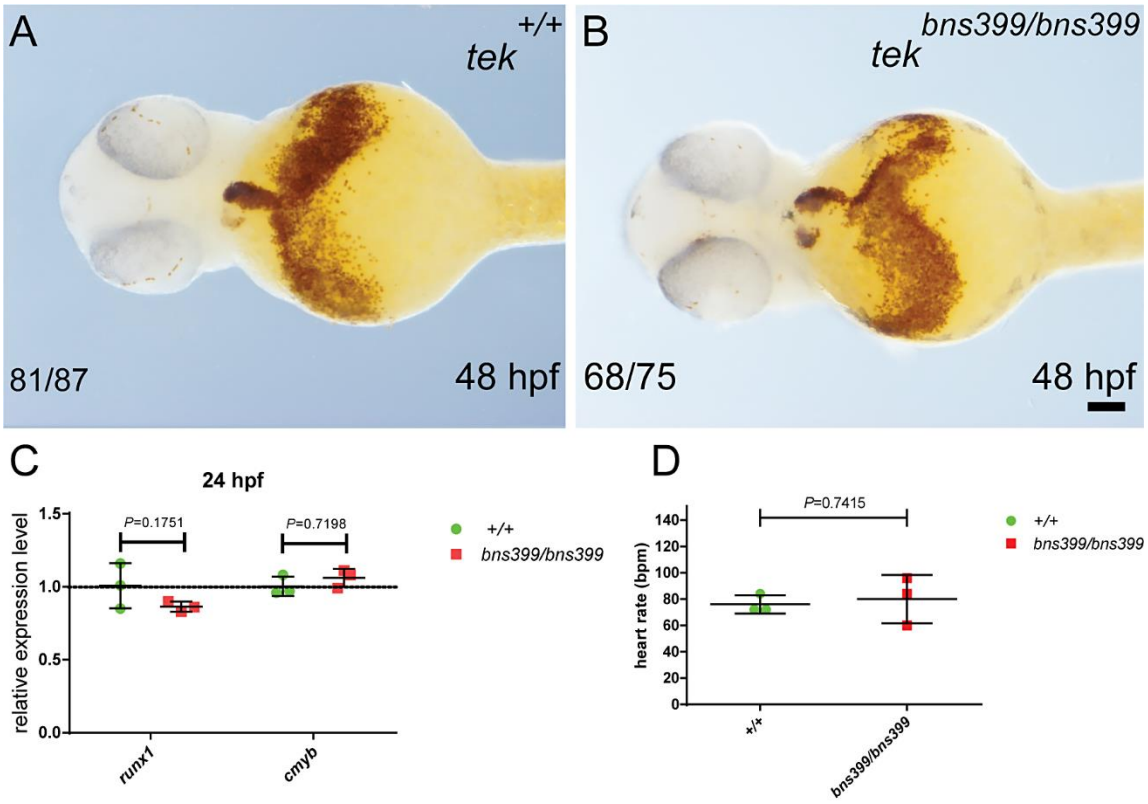

Figure S8. No obvious blood-related phenotypes in *tek*^{bns399} RNA-less mutants.

(A, B) Ventral views of erythrocytes in 48 hpf +/+ siblings (A) and *tek*$^{bns399/bns399}$ embryos (B) stained with O-Dianisidine. (C) *runx1* and *cmyb* mRNA levels in *tek*$^{bns399/bns399}$ mutants when compared to their corresponding +/+ siblings at 24 hpf. (D) Heart rate in 7 mpf *tek*$^{bns399/bns399}$ mutants when compared to their corresponding +/+ siblings. Scale bar: 100 μm.

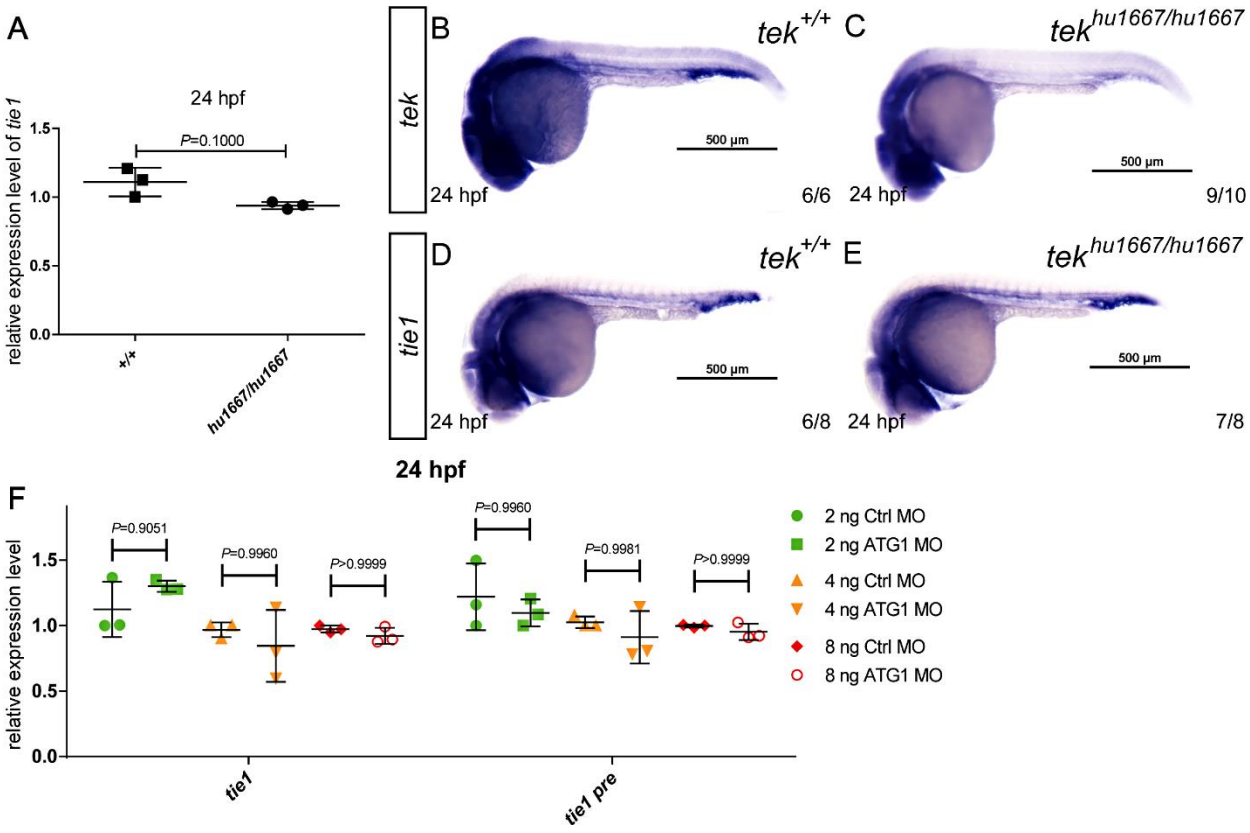

Figure S9. *tie1* does not appear to compensate for the loss of Tek function.

(A) *tek* mRNA levels in *tek*$^{hu1667/hu1667}$ mutants when compared to their +/+ siblings at 24 hpf. (B-E) Expression of *tek (B, C) and tie1 (D, E)*, as detected by wholemount *in situ* hybridization, in 24 hpf *tek*$^{hu1667/+}$ incrossed embryos. (F) *tie1* mRNA and pre-mRNA levels in *tek* ATG1 morphants when compared to control morphants at 24 hpf. In panel A, error bars represent means ± SD (by Mann-Whitney *U* test). In panel F, error bars represent means ± SD (by Two-way analysis of variance (ANOVA) followed by Tukey's HSD test). Scale bars: 500 µm.

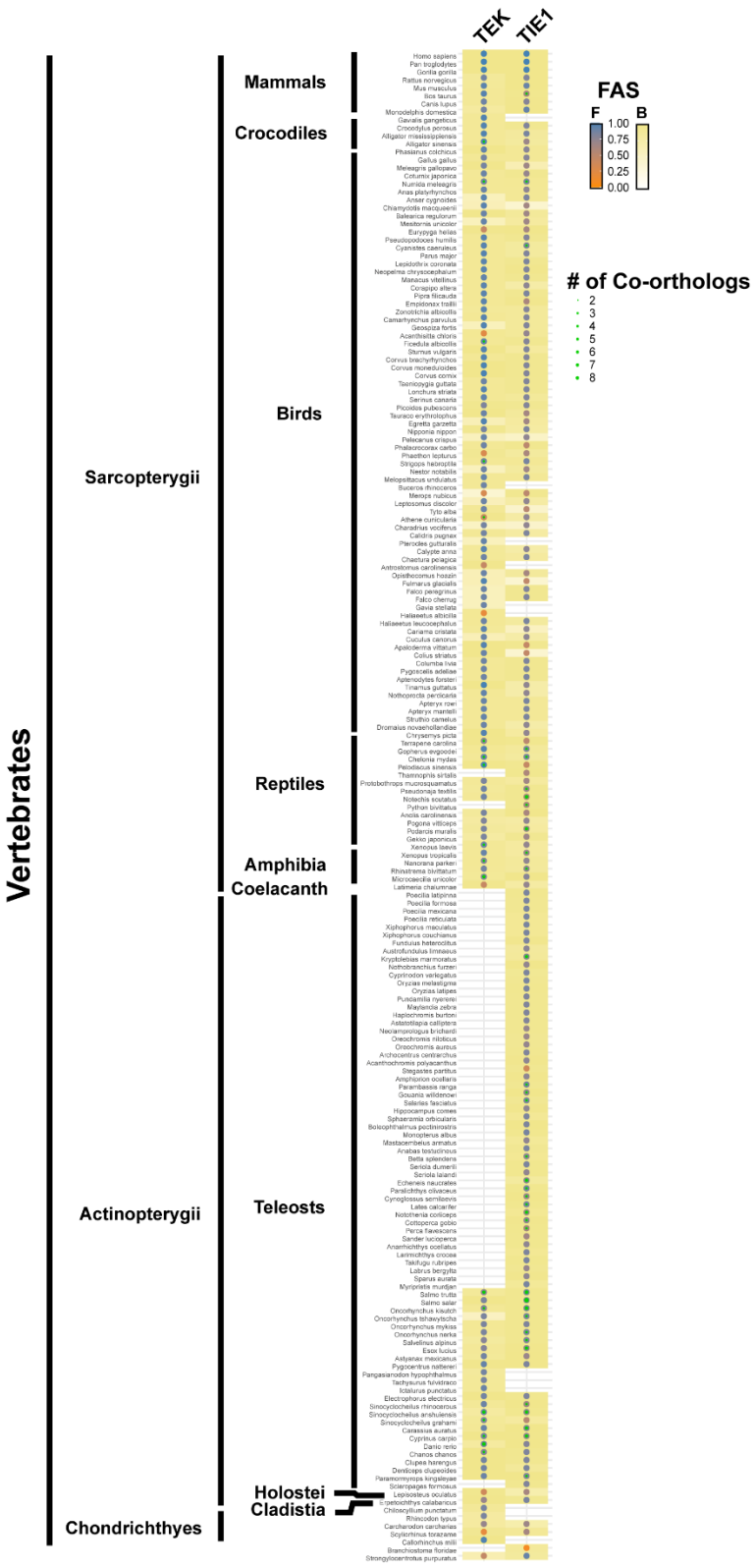

Figure S10. Phylogenetic profile of TEK and TIE1 on a species level resolution.

A dot represents the detection of an ortholog to human TEK or TIE1 in the corresponding species. Inner green circles indicate the presence of co-orthologs to the human protein where the size of the circle represents the number of co-orthologs. Dot colour and cell colour represent the feature architecture similarity score between two orthologs using the human protein (dot colour) and the ortholog (cell colour) as reference, respectively. The data underlying this plot are available in supplementary file 2.

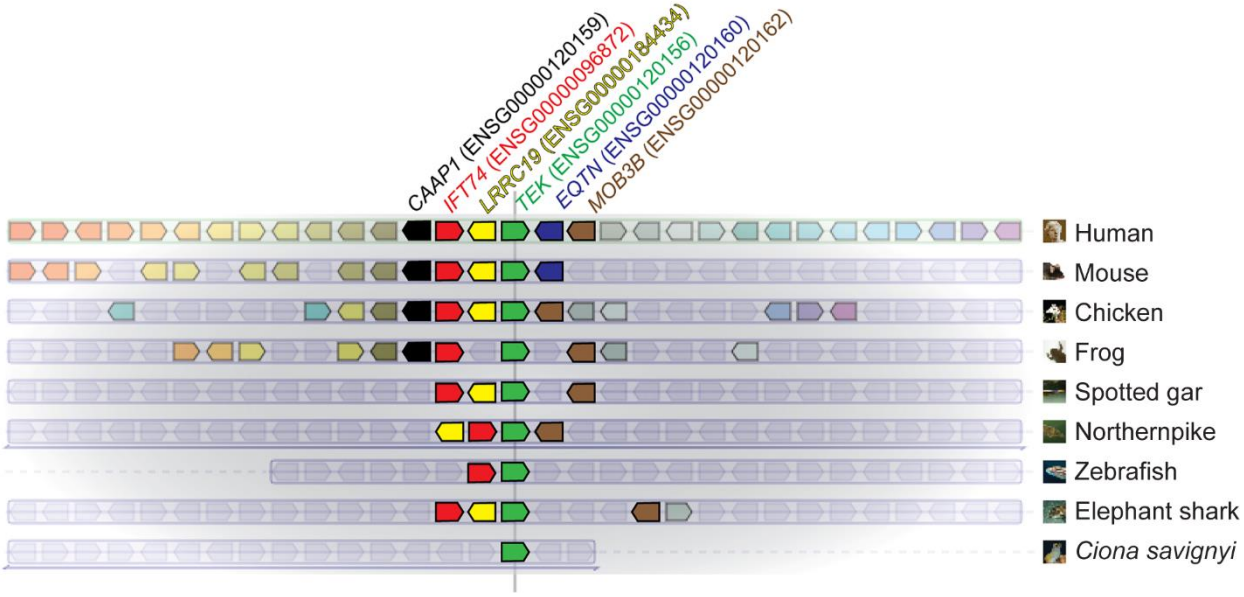

Figure S11. Gene order around the *Tek* locus in various species.

PhyloView representation of *TEK* in the human genome and its orthologs in other genomes. *TEK* and its orthologs are positioned in the centre aligned with their neighbouring genes in various genomes. Genes of the same colour represent orthologs. The location of *ift74* (marked in red), as a direct upstream neighbour of *tek* in the zebrafish genome, is widely conserved amongst different vertebrate species.

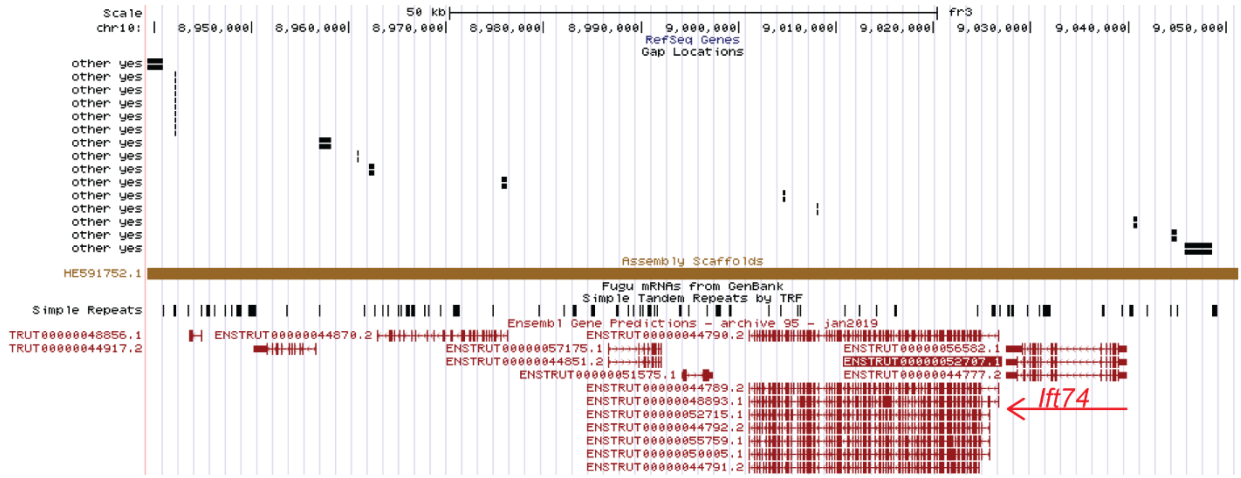

Figure S12. Genomic region distal to *ift74* in fugu.

ift74 is located to the far right of the plot (ENSTRUT00000052707). Downstream of *ift74*, in the direction of its transcription, five additional genes are annotated, none of which resembles a *Tek*-like gene. Only very few and small assembly gaps exist in this region (black blocks), and most of them overlap with other annotated genes. These data suggest that the absence of *Tek* in this species cannot be explained by an assembly artefact. The data shown represent the UCSC Genome Browser on the Fugu Oct. 2011 (FUGU5/fr3) Assembly (https://genome.ucsc.edu).

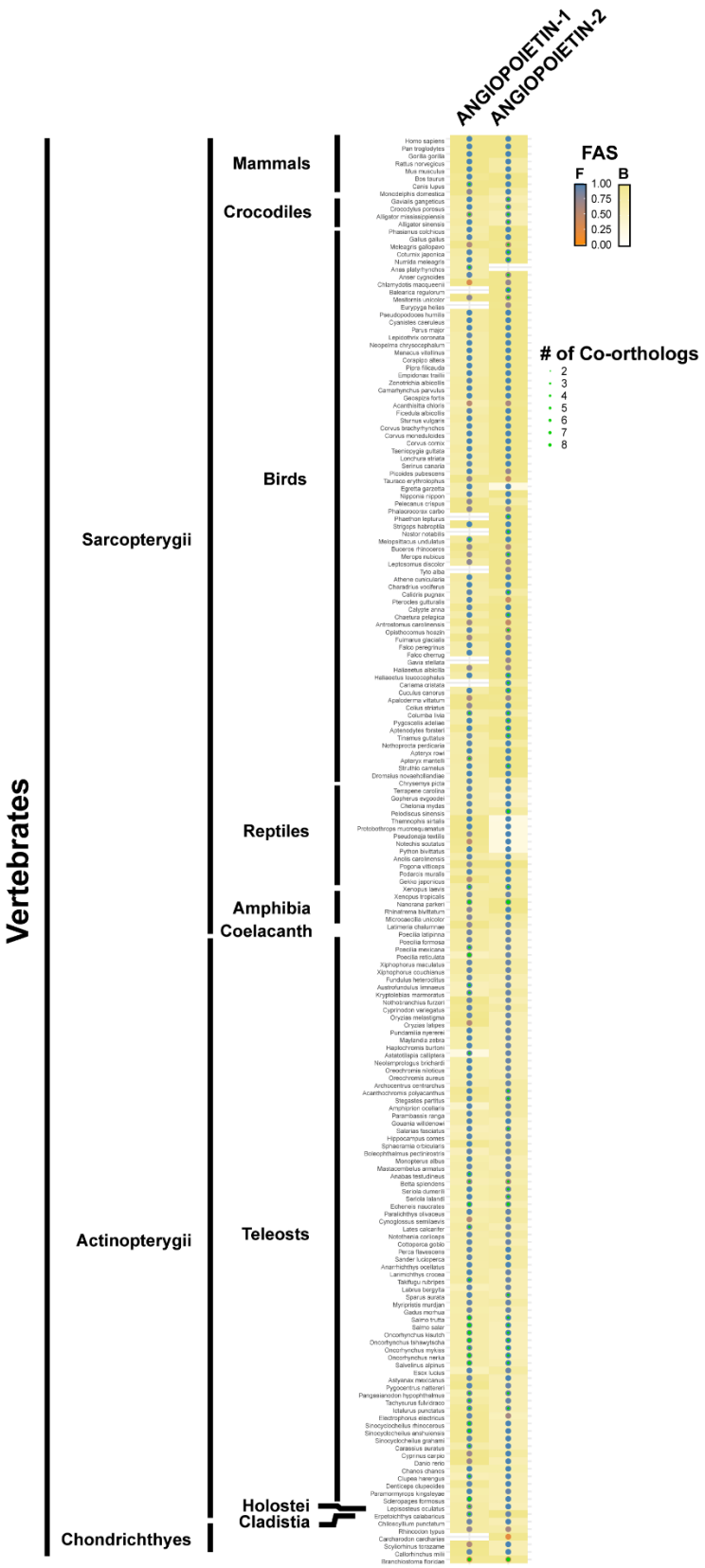

Figure S13. Phylogenetic profile of Angiopoietin-1 and Angiopoietin-2 on a species level resolution.

A dot represents the detection of an ortholog to human Angiopoietin-1 or Angiopoietin-2 in the corresponding species. Inner green circles indicate the presence of co-orthologs to the human protein where the size of the circle represents the number of co-orthologs. Dot colour and cell colour represent the feature architecture similarity score between two orthologs using the human protein (dot colour) and the ortholog (cell colour) as reference, respectively. The data underlying this plot are available in supplementary file 2.

A Feature architecture of human TIE1

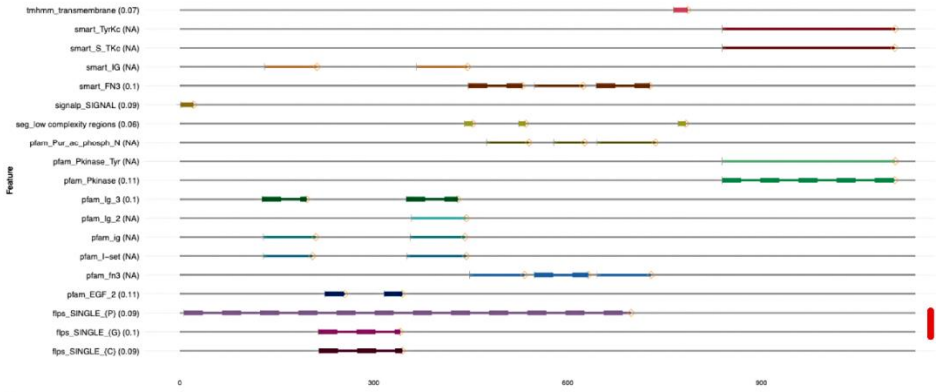

B

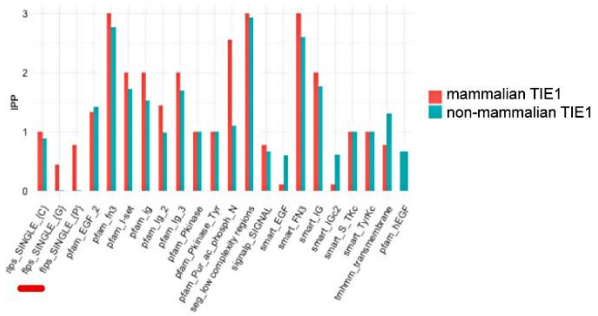

C Feature architecture of human TEK

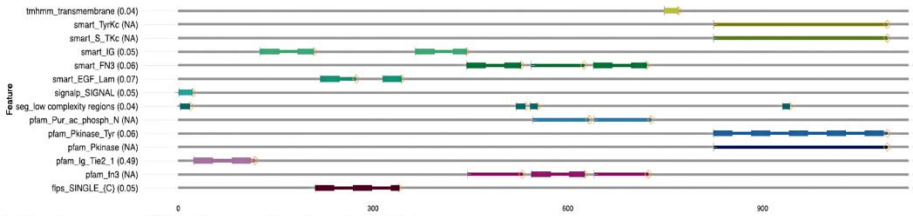

D Feature architecture of zebrafish Tek

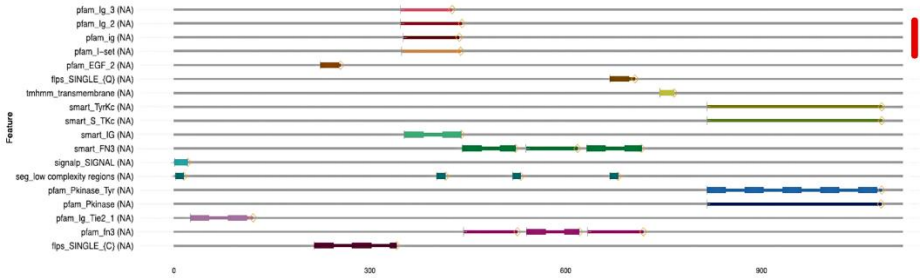

E

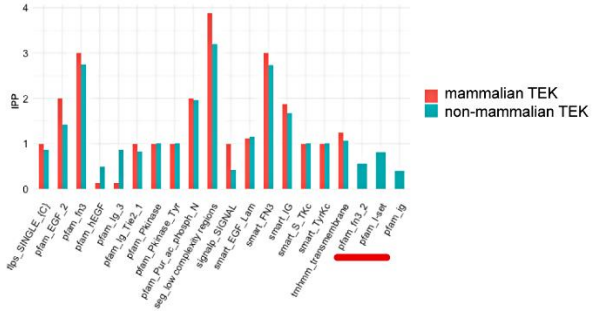

Figure S14. Protein feature architecture of the TIE family receptors has changed on the mammalian lineage.

(A) Schematic representation of human TIE1 protein feature architecture. (B) Comparison of protein feature architecture between mammalian and non-mammalian TIE1 orthologs reveals that mammalian TIE1 harbours a proline and glycine-rich N-terminus (corresponding features are highlighted with red lines). (C) Schematic representation of human TEK protein feature architecture. (D) Schematic representation of zebrafish Tek protein feature architecture. (E) Comparison of feature architecture between mammalian and non-mammalian TEK orthologs reveals that mammalian TEK has a unique Ig2 domain architecture (corresponding features are highlighted with red lines). In panels A, C and D, the numbers next to each protein feature represent the weight of the respective features during scoring of the feature architecture similarity. In the case of overlapping PFAM and SMART domains, we selected the domain that maximizes the similarity score between the two proteins; the weight of the corresponding features was set to 'N.A.'. IPP: Feature instances per protein.

Table S1.

Click here to Download Table S1

Table S2.

Click here to Download Table S2

Table S3.

Click here to Download Table S3

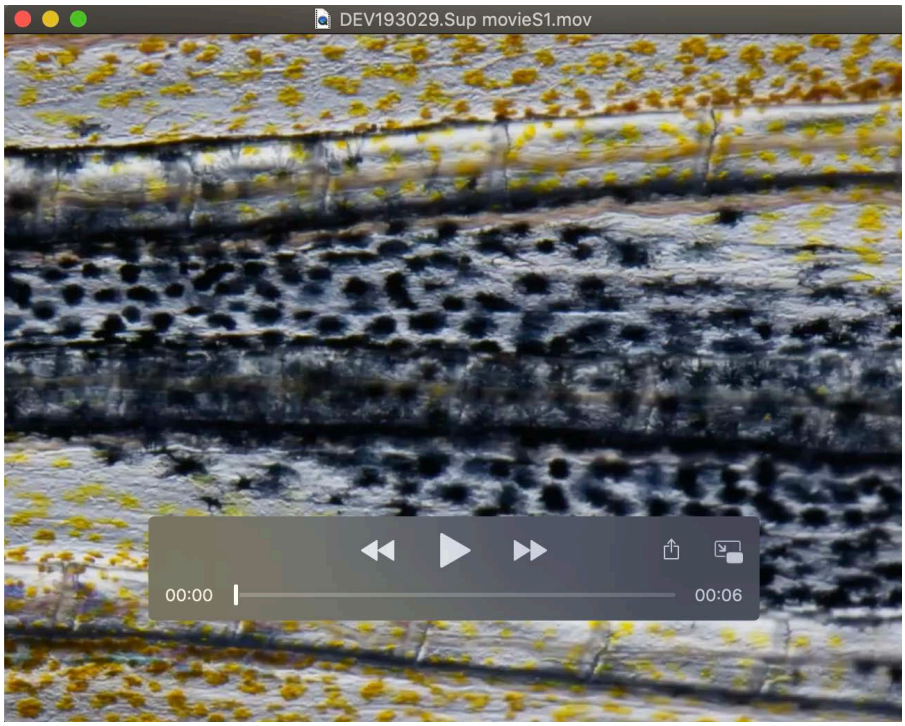

Movie 1. fin blood flow in WT

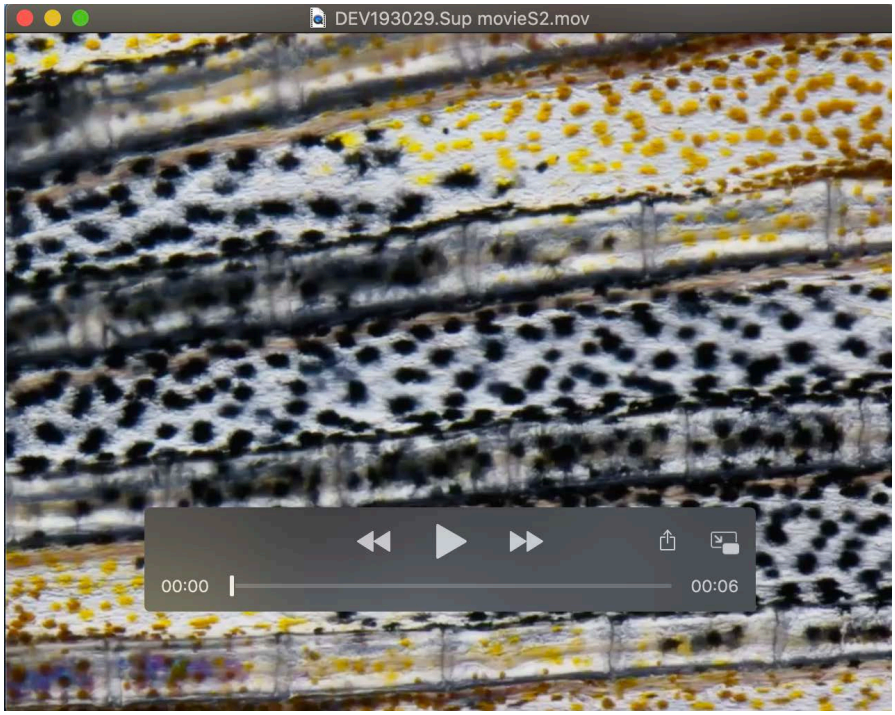

Movie 2. fin blood flow in mutant

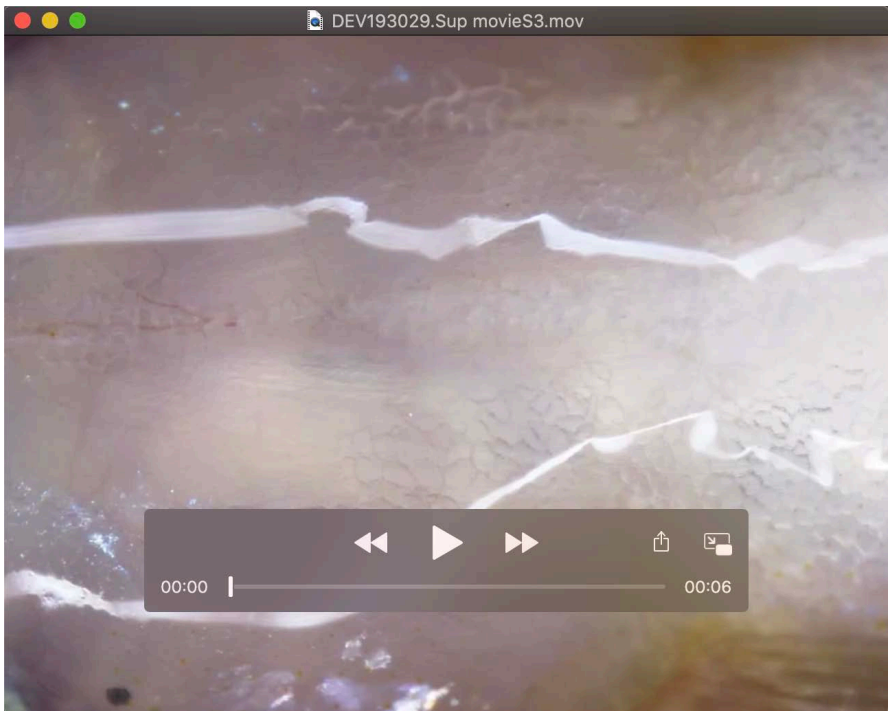

Movie 3. heartbeat in WT

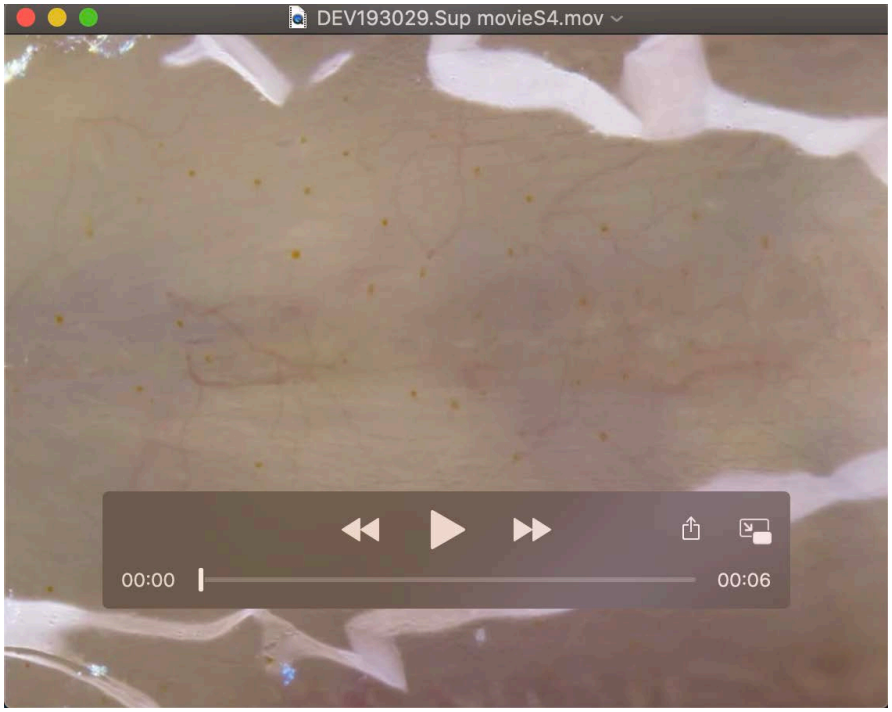

Movie 4. heartbeat in mutant